

Automated synchrogram analysis applied to heartbeat and reconstructed respiration

Claudia Hamann,¹ Ronny P. Bartsch,² Aicko Y. Schumann,³ Thomas Penzel,⁴ Shlomo Havlin,² and Jan W. Kantelhardt³

¹*Institut für Physik, Technische Universität Ilmenau, 98684 Ilmenau, Germany*

²*Department of Physics and Minerva Center, Bar-Ilan University, Ramat Gan 52900, Israel*

³*Institute of Physics, Martin-Luther-Universität Halle-Wittenberg, 06099 Halle (Saale), Germany*

⁴*Schlafmedizinisches Zentrum der Charité Berlin, 10117 Berlin, Germany*

(Received 4 December 2008; accepted 17 February 2009; published online 31 March 2009)

Phase synchronization between two weakly coupled oscillators has been studied in chaotic systems for a long time. However, it is difficult to unambiguously detect such synchronization in experimental data from complex physiological systems. In this paper we review our study of phase synchronization between heartbeat and respiration in 150 healthy subjects during sleep using an automated procedure for screening the synchrograms. We found that this synchronization is significantly enhanced during non-rapid-eye-movement (non-REM) sleep (deep sleep and light sleep) and is reduced during REM sleep. In addition, we show that the respiration signal can be reconstructed from the heartbeat recordings in many subjects. Our reconstruction procedure, which works particularly well during non-REM sleep, allows the detection of cardiorespiratory synchronization even if only heartbeat intervals were recorded. © 2009 American Institute of Physics.

[DOI: [10.1063/1.3096415](https://doi.org/10.1063/1.3096415)]

About one-third of our life we spend sleeping. Since sleep is required for recreation, a disturbed sleep negatively affects our daily physical and mental fitness. However, at least 10% of the human population in the industrialized world suffer from sleep related disorders or sleep-wake dysfunctions. Investigating human physiology during sleep is of high interest not only for identifying sleep related disorders but also for detecting and understanding changes in sleep patterns related to other diseases such as, e.g., Alzheimer or Parkinson disease. The standard procedure in a hospitals' sleep laboratory includes full night polysomnography, where many sensors and electrodes are attached to the patient's body in order to measure heartbeat, respiration, muscle activity, brain waves, and eye movements. Although the major aim of these measurements is to monitor natural sleeping behavior, sleep is often disturbed by the unfamiliar environment and the distemping measuring devices. In contrast, the electrocardiogram (ECG) can be recorded with portable, rather inexpensive and comfortable Holter recorders. In this paper we explore the possibility of extracting respiration signals from ECG recordings by taking advantage of the variation in heart rate during a respiratory cycle ("respiratory sinus arrhythmia"). Based on therewith extracted respiration signals, we study the phase relationship between respiration and heartbeat ("cardiorespiratory synchronization") utilizing an automated procedure for screening cardiorespiratory synchrograms, and find that cardiorespiratory synchronization differs significantly between the main sleep stages. Reconstructed respiration from ECG together with the automated synchrogram analysis might pave the way for assessing sleep and sleep disorders by simply analyzing Holter recordings.

I. INTRODUCTION

Transitions in the synchronization behavior of two coupled oscillators have been shown to be important characteristics of model systems.¹ It has been found that noise, when applied identically to different nonlinear oscillators, can induce, enhance, or destroy synchronization among them.²⁻⁴ However, phase synchronization is difficult to study in experimental data, which are very often inherently nonstationary and thus contain only quasiperiodic oscillations. Among the few recent experimental studies are coupled electrochemical oscillators,³ laser systems,⁴ and climate variables.⁵ Moreover, the question of detecting synchronization between several interacting processes with different time scales in univariate signals has been addressed⁶ and methods for characterizing two different types of phase locking, soft and hard phase locking, and its detection by analyzing univariate data were suggested.⁷

In physiology, the study of phase synchronization focuses on cardiorespiratory data and encephalographic data.⁸ First approaches for the study of cardiorespiratory synchronization have been undertaken by the analysis of the relative position of inspiration within the corresponding cardiac cycle.⁹ More recently, phase synchronization between heartbeat and breathing has been studied during wakefulness using the synchrogram method.¹⁰⁻¹³ While long synchronization episodes were observed in athletes and heart transplant patients (several hundreds of seconds),^{11,12} shorter episodes were detected in normal subjects (typical duration less than hundred seconds).¹²⁻¹⁴ For two recent models of cardiorespiratory synchronization, see Ref. 15.

The cardiorespiratory system consisting of the heart, the blood vessels as well as the lungs plays a major role in hu-

man physiology. Therefore, it has been studied extensively during the past decades. Most approaches covered monovariate analysis of either heartbeat or breathing signals, e.g., employing spectral methods to investigate heart rate variability^{16,17} or exploring correlation behavior and fluctuations by applying detrended fluctuation analysis,^{18–20} or recently phase rectified signal averaging.²¹ Cross modulations and cross interactions between the components of the cardiorespiratory system have been studied by means of cross-correlation analysis, transfer function analysis, (phase) synchronization analysis, and more recently by bivariate phase rectified signal averaging (see Ref. 22 and references therein). In this work, we review our automated synchrogram based procedure²³ using the concept of phase synchronization^{10–13} and study interactions between cardiac and respiratory oscillations under different physiological conditions.

Usually, the cardiorespiratory system is continuously influenced and altered by its environment, e.g., we respond to external stimuli such as sonic or visual input and are sensitive to mental stress. However, during sleep the cardiorespiratory system is self-sustained, reflecting the intrinsic characteristics of the autonomous nervous system and the subjects' physiology. In order to obtain reliable experimental evidences of transitions in phase synchronization behavior, we have thus considered cardiorespiratory synchronization in humans during sleep.²³ It is well known that healthy sleep consists of approximately five cycles of roughly 1–2 h duration. Each cycle usually evolves from non-rapid-eye-movement (non-REM) sleep, consisting of light and deep sleep, to REM sleep.²⁴ Homogeneous long-term data for well-defined conditions of a complex physiological system are thus available from sleep laboratories.²⁵ Investigating human physiology during sleep is of diagnostic value not only for sleep related diseases such as sleep apnea. It can also enhance the understanding and identification of nonsleep related diseases.

We have found the intriguing result that during REM sleep cardiorespiratory synchronization is suppressed by approximately a factor of 3 compared with wakefulness.²³ On the other hand, during non-REM sleep, it is enhanced by a factor of 2.4, again compared with wakefulness. In addition, we have found that these significant differences between synchronization in REM and non-REM sleep are very stable and occur in the same way for males and females, independent of age and independent of the body mass index (BMI). Our results regarding synchronization efficiency suggest that the synchronization is mainly due to a weak influence of the breathing oscillator upon the heartbeat oscillator, which is disturbed in the presence of long-term correlated noise, superimposed by the activity of higher brain regions during REM sleep.

While heartbeat data can be measured easily and conveniently by employing portable devices, the recording of brain waves (electroencephalogram, EEG) and respiration is technically much more difficult. Usually, respiration is measured by either one of the following rather uncomfortable and encumbering and/or invasive and thus ambulatory ill suited methods: (i) by using stretch sensors embedded in a belt and

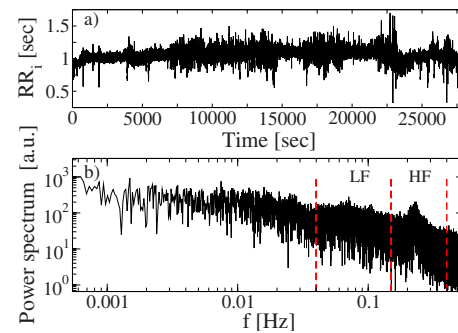


FIG. 1. (Color online) (a) Heartbeat interval time series RR_i from a healthy young subject during sleep. (b) Power spectrum of the signal shown in (a). The LF band (0.04–0.15 Hz) is assumed to reflect blood pressure oscillations, whereas the HF band (0.15–0.4 Hz) reflects respiration via the RSA effect. It can thus be used to reconstruct the respiratory signal.

attached to the chest and/or abdomen surveying excursions and motions of the body surface, (ii) by means of a thermistor and/or a spirometer (flow meter) incorporated in a mouthpiece, a nose clamp or a breathing mask covering the whole nose-mouth area, (iii) by expensive inductive plethysmographs or respiratory magnetometers, or (iv) by impedance pneumography based on impedance cardiographic signals.²⁶ The major aim of polysomnographic measurements²⁷ is to monitor natural sleeping behavior of the patient. However, sleep can be disturbed significantly in a sleep laboratory because of the unfamiliar environment and the distemping measuring devices, both resulting in additional physical and mental stress. We thus explore in this paper a possibility for the reconstruction of respiratory signals from heartbeat intervals since heartbeat can be recorded at home with portable devices.

Our reconstruction algorithm is based on the physiological phenomenon that respiration influences the sympathetic autonomous nervous system. While inspiration enhances sympathetic components followed by an increase in heart rate, expiration suppresses sympathetic and activates vagal components resulting in a heart rate decrease. This variation in the heart rate during the respiratory cycle is generally known as respiratory sinus arrhythmia (RSA). It is important to note that RSA is *not* equivalent to cardiorespiratory synchronization. While RSA only leads to a cyclical variation of heart rate, cardiorespiratory synchronization is only observed when a constant number of heartbeats occur at the same instantaneous phases within the breathing cycle for a period of several consecutive breaths. Both phenomena can occur independent of each other, although an increased RSA might reduce cardiorespiratory synchronization.¹¹

In spectral analysis of heartbeat interval data (see Fig. 1), two prominent peaks are often observed corresponding to characteristic frequency components in the low frequency (LF) (0.04–0.15 Hz) and high frequency (HF) (0.15–0.4 Hz) bands.¹⁶ The LF band has been associated with sympathetic activation; the corresponding peak might be related with blood pressure oscillations (Mayer waves). The HF band is related with vagal components, and it has been shown that HF spectral power is significantly influenced by breathing volume and breathing rate, i.e., changing the breathing pat-

tern alters the HF spectral components.²⁸ Therefore, respiratory components can be extracted from a heartbeat interval time series by Fourier filtering, i.e., applying a band-pass filter adjusted to HF components. This way, we use the RSA effect for the reconstruction of the respiration signal from heartbeat intervals.

The paper is structured as follows. Section II describes our data recordings and the data preprocessing for studying phase synchronization. This includes the reconstruction of respiration signals from heartbeat signals. In Sec. III we describe our phase synchronization analysis for real and reconstructed respiration as well as our automated procedure for the detection of phase synchronization. In Sec. IV we apply this procedure to study cardiorespiratory synchronization.

II. DATA AND DATA PREPARATION

Our studies are based on data collected in the framework of the EU project SIESTA from seven European sleep laboratories.²⁵ The data consist of full night polysomnographic recordings^{27,29} from 150 healthy subjects (age: 50.3 ± 19.4 y) recorded during one regular night (an adaption night was preceding each recording night). Note that for this manuscript we have increased the number of subjects to 150 compared with our original publication²³ where we only considered 112 subjects, and which are a subset of the 150 subjects analyzed here. The average duration of the recordings is 7.9 ± 0.4 h. Based on visual inspection of the recordings and following international standards,²⁴ sleep stages were identified and assigned in intervals of 30 s. Sleep stage classifications include REM sleep (stage 5) and non-REM sleep, i.e., light sleep (stages 1 and 2) and deep sleep (stages 3 and 4) with some additional shorter wake periods.

In this paper we study a one channel electrocardiogram (ECG) signal as well as the oronasal airflow signal measured by a thermistor. Depending on the laboratory, the ECG signal was sampled at 100, 200, or 256 Hz, while airflow was sampled at 16, 20, 100, or 200 Hz. From the raw ECGs we detected the time positions of heartbeats (R peaks) applying either a wavelet based peak detector or a peak detector designed at the German Heart Center and Klinikum Rechts der Isar Munich, Germany.³⁰ We have validated the comparability of both detectors by statistical tests, considering 20 randomly chosen subjects. For an extensive review on ECG beat detection, we refer to Ref. 31. In the next step we derived the series of time intervals between each two successive heartbeats (RR intervals). These series usually contain some artifacts caused by incorrectly detected beat positions, measurement errors, or subject movements. To eliminate these artifacts, we removed beat-to-beat intervals smaller than 300 ms, larger than 2000 ms, or differing by more than 1000 ms from the preceding or the following beat-to-beat interval. Removed data points were linearly interpolated in order to preserve the timing.

Regarding respiration, we studied two types of signals: (i) respiration obtained directly from oronasal airflow and (ii) respiration reconstructed from heartbeat intervals. Noise in oronasal airflow data consists mainly of spikes (outliers) in the quite sinusoidal signal. A simple threshold filter is thus sufficient. All data points exceeding a threshold of 95% of

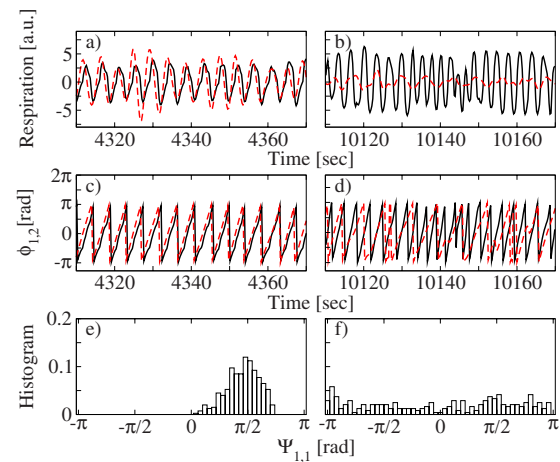


FIG. 2. (Color online) Analysis of respiration signals. (a) and (b) Recorded oronasal airflow (black solid line) is compared with the respiratory signals reconstructed from heartbeat (red dashed lines) for two segments of a recording from a healthy subject. (c) and (d) Instantaneous phases calculated from the oronasal airflow [$\phi_1(t)$, black solid line] and from the reconstructed respiration [$\phi_2(t)$, red dashed line] are compared for the same segments. (e) and (f) Histogram of the phase differences $\phi_1(t) - \phi_2(t)$ between real and reconstructed respiration signals. The peak in (e) indicates that the reconstructed signal resembles the original signal with an unimportant systematic phase shift of approximately $\pi/2$. The uniform distribution in (f) indicates that the respiratory signal could not be reconstructed probably due to a diminished influence of the breathing upon the heartbeat signal, i.e., very weak RSA.

the maximum value or dropping below 95% of the (negative) minimum value within a moving time window are clipped to the corresponding threshold value. After filtering, respiration was resampled at 4 Hz, preparing the signal for phase detection via Hilbert transform. The reason for the selection of this sampling rate lies in the optimal number of 10–20 data points per oscillation for the Hilbert transform of noisy periodic signals. The resampling is done by dividing the original sampling rate by 4 Hz and averaging the corresponding number of data points.

To reconstruct an alternative respiration signal from heartbeat, we began with resampling the beat-to-beat interval series in equidistant time steps. This means we linearly interpolated between the RR_i values occurring at times $t_k = \sum_{i=1}^k RR_i$. We chose a time resolution of 0.25 s corresponding to the 4 Hz of the original respiration signal for comparability. Then, respiration is reconstructed by band-pass Fourier filtering, i.e., calculating the fast Fourier transform (FFT) of the heartbeat interval signal, setting all Fourier coefficients outside the desired HF band (0.15–0.4 Hz) to zero, and calculating the inverse FFT. Two illustrative examples of the reconstructed respiration and the corresponding filtered oronasal airflow signals are shown in Figs. 2(a) and 2(b). In order to investigate and quantify the reconstruction quality of the respiratory signal, we subdivided all signals into segments corresponding to different sleep stages and employed methods of phase-synchronization analysis (see below).

III. ANALYSIS METHODS

In this section we review our automated synchrogram method to study phase synchronization between a continuous

signal (respiration) and a point-process (heartbeats), which we briefly introduced in Ref. 23. In addition, we describe the method we applied to investigate synchronization between measured oronasal airflow and ECG based reconstructed respiration.

A. Calculating and testing instantaneous respiratory phases

In order to study phase synchronization between two signals, it is necessary to obtain instantaneous phases at least for the slower oscillating signal, i.e., for respiration in our case. For a real valued continuous signal $x(t)$, this can be done within an analytic signal approach, adding a corresponding imaginary part $i\tilde{x}(t)$ to the signal. $\tilde{x}(t)$ is calculated by employing Hilbert transform,^{32,33}

$$\tilde{x}(t) = \frac{1}{\pi} \text{PV} \int_{-\infty}^{\infty} \frac{x(t')}{t-t'} dt', \quad (1)$$

where PV denotes the Cauchy principal value. In practice, for homogeneously sampled signals, the Hilbert transform can easily be calculated by the following steps: (i) applying FFT to the original signal $x(t)$, (ii) multiplying the spectral coefficients by $-i \text{sgn}(f)$ with frequency f , and (iii) transforming the manipulated signal back into time domain by applying inverse FFT. Finally, instantaneous phases can be defined from real and imaginary parts of the analytical signal, $\phi(t) = \arctan[\tilde{x}(t)/x(t)]$. Additionally, a sign logic has to be implemented to obtain values $-\pi < \phi \leq \pi$ rather than just $-\pi/2 < \phi \leq \pi/2$ (note that this is available as `atan2` in most computer libraries). Note further that a Hilbert transform requires a rather narrow-banded input signal,^{10,33} and thus a suitable band-pass filter might have to be applied before the transform. Our resampling of the respiration signals at 4 Hz represents an easy implementation of a low pass filter eliminating HF components that would disturb the phase calculations.

Figures 2(a) and 2(b) show two exemplary parts of both, recorded respiration and ECG based reconstructed respiration. The corresponding instantaneous phase signals obtained from Hilbert transforms are shown in Figs. 2(c) and 2(d). It is clearly seen that the reconstruction works well in the section shown in parts (a) and (c), while it completely fails in the section shown in (b) and (d). In order to quantify the quality of the reconstruction, we have plotted in Figs. 2(e) and 2(f) the histograms of the corresponding phase differences.

If recorded and reconstructed respiration signals resemble each other, they exhibit 1:1 phase synchronization and the histogram is strongly peaked. For not synchronized signals, on the other hand, all phase differences have identical probability and the histogram is flat. This can be computationally checked either by calculating standard synchronization indices¹⁰ or by a direct study of the histograms. However, we find that the standard indices strongly depend on the noise level in the signal, sudden phase jumps, and artifacts. In addition, they do not fully vanish for unsynchronized surrogate data, e.g., for reconstructed respiration from one subject and the measured oronasal airflow from another. We thus decided to classify the histograms exemplified in

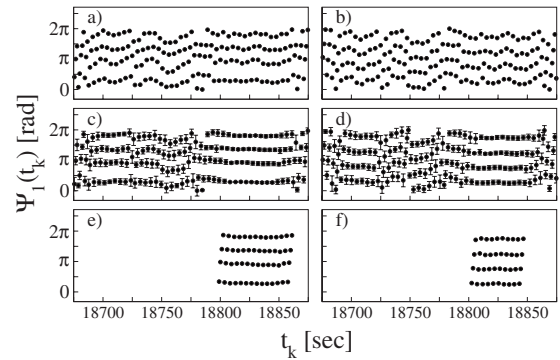


FIG. 3. Examples illustrating the automated synchrogram method for real- (left) and reconstructed (right) respiration signals. Symbols in (a) and (b) show the instantaneous respiratory phases at the time of the heartbeats. (c) and (d) means and standard deviations of the phases, calculated in time intervals of length $\tau=30$ s around each point in the horizontal lines. (e) and (f) Phase points with a standard deviation larger than the threshold were deleted and then sequences shorter than the threshold T were also deleted. Note that T must be slightly smaller for reconstructed breathing (right) since the continuous segments are shorter.

Figs. 2(e) and 2(f) by calculating the mean phase differences $\Delta\phi_\nu = \langle \phi_1(t) - \phi_2(t) \rangle_\nu$ and the corresponding standard deviations within windows ν with length of 30 s, i.e., 120 data points. We define both signals as synchronized if the standard deviation is below 0.5 rad. In this way, we obtain for each subject the overall percentage of synchronized windows for the whole night as well as separately for wake, REM sleep, and non-REM sleep (cf. Table I).

B. Automated phase-synchrogram analysis

In order to study phase synchronization between heartbeat intervals and either the recorded oronasal airflow or the reconstructed respiration signal, we employ the method of phase-synchrogram analysis. This method is ideal for studying phase synchronization between a point process (here, heartbeat) and a continuous signal (here, respiration). While cardiorespiratory synchrograms are traditionally analyzed by visual inspection, we recently suggested a completely automated approach.²³

First, instantaneous phases $\phi_1(t)$ and $\phi_2(t)$ are calculated for both respiratory time series (see Sec. III A). Second, we calculate cumulative respiratory phases $\Phi_j(t) = \phi_j(t) + 2\pi n$, $j=1,2$, starting with $n=0$ and incrementing n if the instantaneous phase $\phi_j(t)$ drops by a value larger than π . Ideally, a new breathing cycle would start with a drop in phase by 2π . However, smaller values occur in practice due to limited time resolution, noise, etc. In rare cases, when the instantaneous phase increases by more than π , n is decremented.

The cardiorespiratory synchrogram is then obtained by mapping the times $t_k = \sum_{i=1}^k RR_i$ of the heartbeats onto the continuous cumulative phases $\Phi_j(t)$. Figures 3(a) and 3(b) illustrate two representative parts of the corresponding synchrograms for measured oronasal airflow (a) and reconstructed breathing (b). In these synchrograms for studying synchronization of n heartbeats within one breathing cycle ($n:1$ synchronization), $\Psi_{1,j}(t_k) = \Phi_j(t_k) \bmod 2\pi$ is plotted versus t_k . In areas with $n:1$ phase synchronization, n parallel horizontal lines appear. The lines vanish if synchronization breaks

down. Figures 3(a) and 3(b) show events of 4:1 phase synchronization. The similarities between (a) and (b) indicate a good reconstruction quality in the considered time window. Arbitrary synchronization ratios $n:m$, i.e., the occurrence of n heartbeats during m breathing cycles, can be studied easily considering synchrograms of $\Psi_{m,j}(t_k) = \Phi_j(t_k) \bmod 2\pi m$ versus t_k and again looking for n parallel horizontal lines.

To study data of many subjects and nights, it is necessary to automatically detect and distinguish synchronized and unsynchronized areas in the synchrograms.²³ We therefore applied a centered moving average filter of window length τ separately for every $r=1, \dots, n$ heartbeats observed within the m considered breathing cycles in the following sense: (i) m breathing cycles, which are assumed to be at the center of the averaging window, are taken and the number n of heartbeats occurring within these m breathing cycles is counted. The times of these heartbeats are denoted as $t_c^{(r)}$, (ii) a regularly spaced phase interval associated with each single heartbeat event at the center position $\Delta\psi_m^{(n)} = 2\pi m/n$ is calculated, (iii) all phases $\psi_m(t_k)$ belonging to neighboring breathing cycles within the time interval $\mathfrak{T}_r = [t_c^{(r)} - \tau/2, t_c^{(r)} + \tau/2]$ are averaged with respect to their dedicated phase range $\mathfrak{R}_r = [(r-1)\Delta\psi_m^{(n)}, r\Delta\psi_m^{(n)}], r=1, \dots, n$,

$$\langle \Psi_m^{(r)} \rangle (t_c^{(r)}) = \frac{1}{N_{\mathfrak{R}_r, t_k \in \mathfrak{T}_r}} \sum \Psi_m^{(r)}(t_k). \tag{2}$$

Here, $N_{\mathfrak{R}_r}$ denotes the number of phases occurring in the time window \mathfrak{T}_r and the phase range \mathfrak{R}_r , as obtained from the synchrogram. Note that even when n heartbeats occur during m breathing cycles at the center position, there might be a different number of heartbeats during other m breathing cycles within the same considered moving average window of width τ . In addition to the average, we calculate for each of the r heartbeats a standard deviation $\hat{\sigma}_r$.

In the next step, every value $\Psi_m^{(r)}(t_k = t_c^{(r)})$ during the centered m breathing cycles is replaced by the corresponding mean value $\langle \Psi_m^{(r)}(t_k) \rangle$, as illustrated for $n=4$ and $m=1$ in Figs. 3(c) and 3(d). In addition, the four different $\hat{\sigma}_r$ are shown as error bars.

In the final step shown in Figs. 3(e) and 3(f) we remove all points in the synchrogram where the condition $\hat{\sigma}_r < 2\pi m/n\delta$ is violated and keep only episodes of constant n that are longer than a minimum period T . From the remaining synchronized episodes, we can determine the percentage of synchronized episodes compared with the total sleep duration.

C. Optimizing synchrogram evaluation parameters

For our automated analysis of phase synchrograms, three parameters needed to be optimized:²³ (i) the (time) width τ of the moving average filter, (ii) the standard deviation limit parameter δ , and (iii) the minimum episode duration T . To perform the optimization, we studied the influence of the parameters on the overall synchronization for total nights, comparing the results for the real data (heartbeat and oronasal airflow) with those for (unsynchronized) surrogate data.

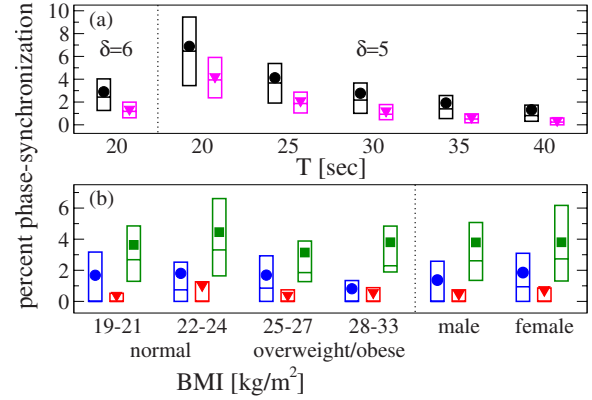


FIG. 4. (Color online) Medians, upper and lower quartiles (bars), and means (filled symbols) for the detected synchronization rates (a) vs T for all original data (black dotted bars and circles) and surrogate data (magenta striped bars and triangles), left of dotted line $\delta=6$, right of dotted line $\delta=5$. (b) The results for optimized parameters (for $\delta=5$ and $T=30$ s) are shown vs BMIs and gender for wakefulness (blue dotted bars and circles), REM sleep (red blank bars and triangles), and non-REM sleep (green striped bars and diamonds). Note the similar synchronization behavior in all subgroups. This figure is based on our original data set of 112 subjects and is adapted from Ref. 23.

The surrogate data were obtained by randomly combining heartbeat data from one subject with breathing data from another subject.

Figure 4(a) shows the total night synchronization percentage for different δ and T . As expected, the largest ratio of synchronized episodes was found for small T and small δ (i.e., a large limit for the standard deviations). However, in this case, a rather large number of synchronized episodes are also reported for the unsynchronized surrogate data. The ratio of the mean percentage of synchronization in real data over the mean percentage in surrogate data increases from 1.6 for $T=20$ s to 3.4 for $T=40$ s. However, for $T=40$ s only very few synchronization episodes were detected. We therefore suggested choosing $\delta=5$ and $T=30$ s to optimize the ratio between correctly detected real synchronization episodes and falsely detected synchronization episodes in surrogate data. Together with $\tau=30$ s, these parameter values provide a good separation and, furthermore, the time parameters coincide with the time interval of 30 s used in sleep stage classification. Note that δ has a similar influence on the results as T (not shown in detail), while τ just weakly effects the results.

When comparing synchronized episodes for real and reconstructed respiration [see Figs. 3(e) and 3(f)], one observes, in general, shorter synchronized episodes for the reconstructed respiration. This is due to instabilities in the reconstruction process. We thus adjusted $T_{rec}=24$ s for reconstructed breathing, keeping both τ and δ at the same values. This led to similar durations of the synchronized episodes in all subjects compared with recorded respiration and $T=30$ s.

IV. RESULTS AND DISCUSSION

A. Phase synchronization with recorded respiration

In this subsection we review our results obtained from 112 subjects from the SIESTA database,²³ which we origi-

nally used to study cardiorespiratory synchronization by applying our automated synchrogram analysis (see Sec. III) to heartbeat and recorded respiratory data. In Secs. IV B and IV C, when studying cardiorespiratory synchronization based on reconstructed respiratory data, we have increased the number of subjects to 150 including all 112 subjects of the previous study.

Calculating the mean, median, and quartiles for the time ratio of phase synchronized episodes separately for wakefulness, REM sleep, and non-REM sleep, we found highly significant differences. During non-REM sleep, we observed phase synchronization during 3.8% of the total time compared with just 0.6% during REM sleep—a difference by a factor of 6.3. Wakefulness during the night—excluding times before the initial sleep onset and after final awakening—was clearly intermediate, since we found 1.6% of it to show cardiorespiratory phase synchronization. Similar differences were observed for other values of T and δ .

We also studied synchronization separately for several groups with different BMIs, and men and women. Figure 4(b) shows that the results are very similar in these subcategories of subjects. The same holds for different age groups,²³ although both heart rate and breathing rate are known to depend on BMI and age. However, when comparing very young and old subjects, one observes a shift to lower values in synchronized episodes during non-REM sleep for older subjects. Altogether, these results prove that our finding of significant differences between the cardiorespiratory synchronization in REM and non-REM sleep is very stable.

Evidence of stable but pronounced differences between REM and non-REM sleep has been reported in the fluctuations of both heartbeat¹⁹ and respiration.²⁰ Influences of the central nervous system (with its sleep stage regulation in higher brain regions) on the autonomous nervous system was suggested to be responsible for these differences. The similarity led us to hypothesize that the diminished synchronization during REM sleep is also caused by influences of the central nervous system. We note that there is very little ($\approx 14\%$) increase in the amplitude of heartbeat or breathing fluctuations during REM sleep when compared with non-REM sleep. The changes in the synchronization behavior can thus not be due to variations in the strength of the influences from the brain. Rather they must be due to the correlation structure imposed by these influences. Long-term correlations are nearly absent in both heartbeat and breathing during non-REM sleep.

We suggested the following physiological mechanism to explain our findings of the sleep stage differences in cardiorespiratory phase synchronization. As long as the heartbeat oscillator and the breathing oscillator (as parts of the autonomous nervous system) are only affected by uncorrelated noise from higher brain regions, they run like two weakly coupled oscillators, and they clearly show synchronization as expected, possibly enhanced by the noise.² However, if the higher brain regions are more active and impose long-term correlated noise on the two oscillators, as is the case during REM sleep, the noise disturbs the emergence of synchronized patterns, leading to a drastic reduction in synchroniza-

TABLE I. Average synchronization between recorded oronasal airflow and ECG based reconstructed breathing within different sleep stages in percent. Results are shown for all subjects and for subject characterized by different relative fluctuations σ of the reconstructed breathing. Numbers in brackets denote the number of considered individuals in the respective group.

	Whole night	Wake	REM	Non-REM
All	30.5(150)	17.9(150)	17.8(149)	35.9(150)
$\sigma \leq 0.2$	47.9 (74)	33.3 (33)	44.0 (33)	52.3 (88)
$\sigma \leq 0.25$	39.5(110)	25.1 (95)	25.5 (95)	44.3(117)
$\sigma \leq 0.3$	33.2(136)	20.6(129)	19.2(137)	37.4(143)

tion episodes. Hence, we suggest from the experimental data that correlated noise rather suppresses synchronization, while uncorrelated noise might increase it.

Our results and interpretations are in agreement with the finding of enhanced cardiorespiratory synchronization in heart transplanted patients, where correlated signals from the brain can hardly affect the heartbeat oscillator.¹² They further affirm the recently reported theory that synchronization pattern can only indirectly be related to cardiac impairments.³⁴ Reduced long-term correlated regulation activity could possibly explain the increase in synchronization in well-trained athletes,¹¹ where fluctuations of heartbeat and breathing might be avoided to optimize the cardiovascular system for optimal performance.

For a discussion of the phase synchronization ratios $n:m$ between oronasal airflow and heartbeat data, we refer to our original paper.²³ There we have shown that mainly $n:1$ synchronization is effective in the cardiorespiratory system.

B. Quality of reconstructed respiration

Now we want to study cardiorespiratory synchronization based solely on heartbeat data. The first step of this task — the reconstruction of respiration from heartbeat time series — has been described in Sec. III A. After the reconstruction, we should make sure that the reconstructed respiration is reliable as in the example shown in Figs. 2(a), 2(c), and 2(e) rather than quite arbitrary as in the example shown in Figs. 2(b), 2(d), and 2(f). We have thus checked for all subjects the reliability of the respiration reconstruction, calculating for each of them the overall percentage of synchronized 30 s windows of real and reconstructed respiration. The procedure described at the end of Sec. III A is performed for the whole nights as well as separately for wake, REM sleep, and non-REM sleep. Average values can be found in Table I.

Figure 5(a) shows the percentage of whole-night synchronization between both respiratory signals as a function of the relative fluctuations σ of the reconstructed respiration. Considering the time intervals between phase increases in 2π in the cumulative reconstructed respiratory phases $\Phi_2(t)$, σ is defined as the quotient of the standard deviation of these breathing intervals over the mean breathing interval. Since the respiratory data is sometimes nonstationary, we calculate σ for windows of $T_\sigma=300$ s and then average these values over the whole night.

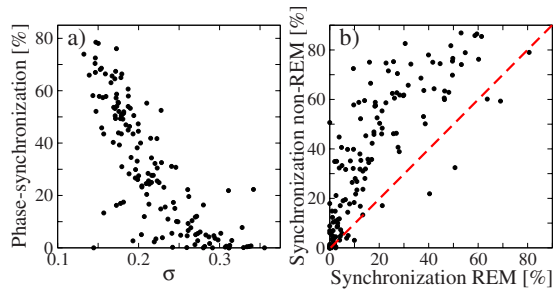


FIG. 5. (Color online) (a) Percentage of synchronized time between real and reconstructed respiration signals vs relative fluctuations σ of the reconstructed respiration for whole nights. Values of σ between 0.2 and 0.3 seem appropriate to exclude subjects with failing reconstruction of respiration. (b) The percentage of synchronized time between real- and reconstructed respiration signals is calculated separately during REM sleep and non-REM sleep, and the pairs of values are plotted in a scatter plot. Since the points for most subjects are above the diagonal (dashed line), the reconstruction is more reliable during non-REM sleep.

Each point in Fig. 5(a) represents one subject from our database. It is obvious that there are subjects where the reconstruction is rather successful (large percentage of correctly, i.e., synchronous reconstructed respiration), while for others it more or less fails. Obviously, the value of σ is usually larger for subjects with failing reconstruction. The relative fluctuations of the reconstructed respiration, i.e., σ , can thus be used as an approximate parameter for the quality of the reconstruction. Consequently, we compare results regarding reconstructed cardiorespiratory synchronization taking into account just subjects with values of σ below given thresholds (see also Table I). We note that we tried to use different parameters characterizing the height of the peak in the HF band of the power spectrum [see Fig. 1(b)] as replacements for σ in classifying good and bad reconstruction of respiration. However, σ turned out to be superior to all these parameters.

Figure 5(b) shows the percentage of synchronization between both respiratory signals during REM sleep versus the corresponding percentage during non-REM sleep in the same subject. Again, each point represents one subject. One clearly observes that well reconstructed respiration is found rather during non-REM sleep than during REM sleep since more subjects are found above the diagonal in Fig. 5(b). This observation is stable for different thresholds for σ (see Table I). Except for $\sigma \leq 0.2$, results for wakefulness and REM sleep are basically the same, also reflecting the well-known statistical resemblance of REM and wake stages.

C. Phase synchronization with reconstructed respiration

Figure 6(a) shows the whole-night percentages of cardiorespiratory synchronization for the real respiration (left subpanel) and the reconstructed respiration (right subpanel) considering subsets of the 150 subjects with σ below and above the indicated thresholds and slightly reduced $T_{\text{rec}} = 24$ s. We have employed the automated synchrogram analysis algorithm described in Sect. III to calculate these percentages of phase synchronization. The close similarity of the results for real and reconstructed respiration prove that car-

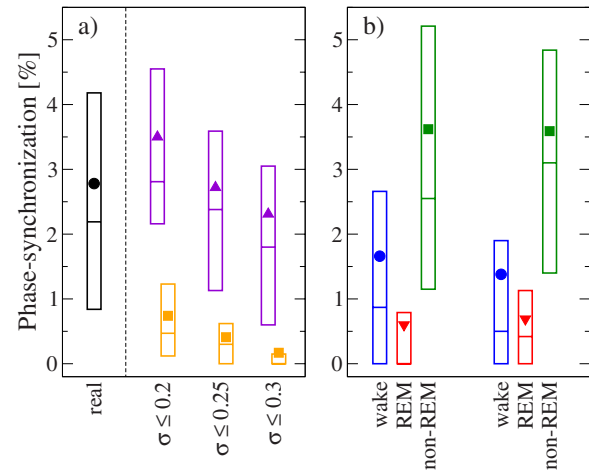


FIG. 6. (Color online) (a) Median, upper and lower quartiles, and mean (dot) of percentage of phase synchronized time regarding heartbeat and real breathing signal (left). The three sets on the right show the results for heartbeat and reconstructed respiration for different σ . The violet striped bars represent the values for subjects with σ below the threshold value and the dark yellow blank bars for breathing signals with σ above the threshold. (b) Cardiorespiratory synchronization percentages for real respiration signals (left set) and reconstructed respiration signals (right set) during different sleep stages (wake=blue, REM=red, non-REM=green).

diorespiratory synchronization can be calculated based solely on heartbeat data. Comparing the values with those in the left subpanel, we think that the limit $\sigma < 0.25$ is most appropriate.

For Fig. 6(b) we have split the data into parts of wakefulness, non-REM sleep, and REM sleep. Again there is a close similarity for the results based on real respiration and reconstructed respiration. The main finding of drastically reduced cardiorespiratory synchronization during REM sleep and enhanced cardiorespiratory synchronization during non-REM sleep compared with wakefulness is fully confirmed.

V. CONCLUSION

We studied cardiorespiratory phase synchronization for a large database of healthy subjects, further increasing the number of subjects considered in our original paper.²³ For this purpose, we developed and thoroughly described an algorithm detecting epochs of synchronization automatically and systematically in synchrogram plots. Comparing the synchronization behavior during different well-defined physiological stages, we observed clearly reduced synchronization during REM sleep and enhanced synchronization during non-REM sleep compared with wakefulness. Since REM and non-REM sleep differ mainly in the type of activity of higher brain centers, it seems probable that the differences in cardiorespiratory synchronization are caused by the more and less long-term correlated regulation actions of the brain during REM and non-REM sleep, respectively.

In addition, we developed and tested a method for the reconstruction of respiration signals from interheartbeat time series based on the RSA effect and the HF spectral component of heartbeat. We have shown that the reliability of the reconstruction can be checked for each subject by calculating the relative standard deviation of the reconstructed breathing intervals. In general, the reconstruction is more reliable dur-

ing non-REM sleep compared with REM sleep. The respiration reconstruction works well in most subjects and yields very similar results for the cardiorespiratory phase synchronization as the recorded respiration data. Hence, a simple Holter recording will be sufficient for the study of cardiorespiratory synchronization in many subjects. The findings should be helpful in the discrimination of sleep stages based only on Holter recordings.

Alternatively, the reconstruction of respiration might be based on the heights of the *R* peaks in multiple lead ECG recordings if such records are available. Possibly, a different reconstruction method can improve the reconstruction quality particularly during REM sleep. Such a method might be combined with the approach studied in this paper. This possibility should be explored in future work. In addition, the consistency of the reconstruction with respiration recorded with stretch sensors could be checked.

ACKNOWLEDGMENTS

We would like to acknowledge financial support from the European Union (project DAPHNet, Grant No. 018474-2), from Deutsche Forschungsgemeinschaft (DFG) (Grant Nos. KA 1676/3 and Pe628/3), and the Adar Foundation for advancing heart research at Bar-Ilan University. C.H. is particularly grateful to the Minerva Foundation for funding her visit to Bar-Ilan University.

- ¹M. G. Rosenblum, A. S. Pikovsky, and J. Kurths, *Phys. Rev. Lett.* **76**, 1804 (1996); E. Rosa, Jr., E. Ott, and M. H. Hess, *ibid.* **80**, 1642 (1998); K. J. Lee, Y. Kwak, and T. K. Lim, *ibid.* **81**, 321 (1998); G. V. Osipov, B. Hu, Ch. Zhou, M. V. Ivanchenko, and J. Kurths, *Phys. Rev. Lett.* **91**, 024101 (2003); Z. Liu, B. Hu, and L. D. Iasemidis, *Europhys. Lett.* **71**, 200 (2005); D. A. Smirnov and R. G. Andrzejak, *Phys. Rev. E* **71**, 036207 (2005); Y.-Ch. Lai, M. G. Frei, and I. Osorio, *ibid.* **73**, 026214 (2006); K. Wood, C. van den Broeck, R. Kawai, and K. Lindenberg, *Phys. Rev. Lett.* **96**, 145701 (2006).
- ²A. Maritan and J. R. Banavar, *Phys. Rev. Lett.* **72**, 1451 (1994); Ch. Zhou and J. Kurths, *ibid.* **88**, 230602 (2002); J. N. Teramae and D. Tanaka, *ibid.* **93**, 204103 (2004); B. Blasius, *Phys. Rev. E* **72**, 066216 (2005); Sh. Guan, Y.-Ch. Lai, and Ch.-H. Lai, *ibid.* **73**, 046210 (2006); S. F. Brandt, B. K. Dellen, and R. Wessel, *Phys. Rev. Lett.* **96**, 034104 (2006).
- ³Ch. Zhou, J. Kurths, I. Z. Kiss, and J. L. Hudson, *Phys. Rev. Lett.* **89**, 014101 (2002); I. Z. Kiss, J. L. Hudson, J. Escalona, and P. Parmananda, *Phys. Rev. E* **70**, 026210 (2004).
- ⁴S. Boccaletti, E. Allaria, R. Meucci, and F. T. Arecchi, *Phys. Rev. Lett.* **89**, 194101 (2002); C. S. Zhou, J. Kurths, E. Allaria, S. Boccaletti, R. Meucci, and F. T. Arecchi, *Phys. Rev. E* **67**, 066220 (2003).
- ⁵D. Maraun and J. Kurths, *Geophys. Res. Lett.* **32**, L15709, DOI: 10.1029/2005GL023225 (2005).
- ⁶N. B. Janson, A. G. Balanov, V. S. Anishchenko, and P. V. E. McClintock, *Phys. Rev. Lett.* **86**, 1749 (2001).
- ⁷A. G. Rossberg, K. Bartholomé, H. U. Voss, and J. Timmer, *Phys. Rev. Lett.* **93**, 154103 (2004).
- ⁸P. Tass, M. G. Rosenblum, J. Weule, J. Kurths, A. Pikovsky, J. Volkman, A. Schnitzler, and H.-J. Freund, *Phys. Rev. Lett.* **81**, 3291 (1998); L. Angelini, M. De Tommaso, M. Guido, K. Hu, P. Ch. Ivanov, D. Marinazzo, G. Nardulli, L. Nitti, M. Pellicoro, C. Pierro, and S. Stramaglia, *ibid.* **93**, 038103 (2004).
- ⁹P. Engel, G. Hildebrandt, and H. G. Scholz, *Eur. J. Physiol.* **298**, 258 (1968); H. Pessenhofer and T. Kenner, *ibid.* **355**, 77 (1975); F. Raschke, in *Coordination in the circulatory and respiratory systems*, in *Temporal Disorder in Human Oscillatory Systems: Proceedings of an International Symposium*, edited by L. Rensing, U. an der Heiden, and M. C. Mackey (Springer, Berlin, 1987), pp. 152–158.
- ¹⁰M. G. Rosenblum, A. Pikovsky, C. Schäfer, P. A. Tass, and J. Kurths, in: *Handbook of Biological Physics*, edited by S. Gielen and F. Moss (Elsevier, New York, 2001), Vol. 4, p. 279; A. Pikovsky, M. Rosenblum, and J. Kurths, *Synchronization—A Universal Concept in Nonlinear Science* (Cambridge University Press, Cambridge, 2001).
- ¹¹C. Schäfer, M. G. Rosenblum, J. Kurths, and H.-H. Abel, *Nature (London)* **392**, 239 (1998); *Phys. Rev. E* **60**, 857 (1999).
- ¹²E. Toledo, S. Akselrod, I. Pinhas, and D. Aravot, *Med. Eng. Phys.* **24**, 45 (2002).
- ¹³M. B. Lotric and A. Stefanovska, *Physica A* **283**, 451 (2000); A. Stefanovska, H. Haken, P. V. E. McClintock, M. Hozic, F. Bajrovic, and S. Ribaric, *Phys. Rev. Lett.* **85**, 4831 (2000); M.-Ch. Wu and Ch.-K. Hu, *Phys. Rev. E* **73**, 051917 (2006).
- ¹⁴M. D. Prokhorov, V. I. Ponomarenko, V. I. Gridnev, M. B. Bodrov, and A. B. Bespyatov, *Phys. Rev. E* **68**, 041913 (2003).
- ¹⁵K. Kotani, K. Takamasu, Y. Ashkenazy, H. E. Stanley, and Y. Yamamoto, *Phys. Rev. E* **65**, 051923 (2002); V. N. Smelyanskiy, D. G. Luchinsky, A. Stefanovska, and P. V. E. McClintock, *Phys. Rev. Lett.* **94**, 098101 (2005).
- ¹⁶Task Force of the European Society of Cardiology and the North American Society of Pacing and Electrophysiology, *Circulation* **93**, 1043 (1996).
- ¹⁷S. Akselrod, D. Gordon, F. A. Ubel, D. C. Shannon, A. C. Barger, and R. J. Cohen, *Science* **213**, 220 (1981); M. Kobayashi and T. Musha, *IEEE Trans. Biomed. Eng.* **BME-29**, 456 (1982); L. Keselbrener and S. Akselrod, *ibid.* **43**, 789 (1996); A. L. Goldberger, D. R. Rigney, and B. J. West, *Sci. Am.* **262**, 42 (1990).
- ¹⁸C.-K. Peng, J. Mietus, J. M. Hausdorff, S. Havlin, H. E. Stanley, and A. L. Goldberger, *Phys. Rev. Lett.* **70**, 1343 (1993); *Physica A* **249**, 491 (1998); L. A. Amaral, A. L. Goldberger, P. Ch. Ivanov, and H. E. Stanley, *Phys. Rev. Lett.* **81**, 2388 (1998); P. Ch. Ivanov, M. G. Rosenblum, L. A. N. Amaral, Z. Struzik, S. Havlin, A. L. Goldberger, and H. E. Stanley, *Nature (London)* **399**, 461 (1999).
- ¹⁹A. Bunde, S. Havlin, J. W. Kantelhardt, T. Penzel, J.-H. Peter, and K. Voigt, *Phys. Rev. Lett.* **85**, 3736 (2000); T. Penzel, J. W. Kantelhardt, L. Grote, J.-H. Peter, and A. Bunde, *IEEE Trans. Biomed. Eng.* **50**, 1143 (2003).
- ²⁰J. W. Kantelhardt, T. Penzel, S. Rostig, H. F. Becker, S. Havlin, and A. Bunde, *Physica A* **319**, 447 (2003); S. Rostig, J. W. Kantelhardt, T. Penzel, W. Cassel, J. H. Peter, C. Vogelmeier, H. F. Becker, and A. Jerrentrup, *Sleep* **28**, 411 (2005).
- ²¹A. Bauer, J. W. Kantelhardt, A. Bunde, P. Barthel, R. Schneider, M. Malik, and G. Schmidt, *Physica A* **364**, 423 (2006); A. Bauer, J. W. Kantelhardt, P. Barthel, R. Schneider, T. Mäkkikallio, K. Ulm, K. Hnatkova, A. Schömig, H. Huikuri, A. Bunde, M. Malik, and G. Schmidt, *Lancet* **367**, 1674 (2006); J. W. Kantelhardt, A. Bauer, A. Y. Schumann, P. Barthel, R. Schneider, M. Malik, and G. Schmidt, *Chaos* **17**, 015112 (2007).
- ²²A. Y. Schumann, J. W. Kantelhardt, A. Bauer, and G. Schmidt, *Physica A* **387**, 5091 (2008).
- ²³R. Bartsch, J. W. Kantelhardt, T. Penzel, and S. Havlin, *Phys. Rev. Lett.* **98**, 054102 (2007).
- ²⁴A. Rechtschaffen and A. Kales, *A Manual of Standardized Terminology, Techniques, and Scoring System for Sleep Stages of Human Subjects* (U.S. Government Printing Office, Washington, 1968).
- ²⁵G. Klosch, B. Kemp, T. Penzel, A. Schlogl, P. Rappelsberger, E. Trenker, G. Gruber, J. Zeithofer, B. Saletu, W. M. Herrmann, S. L. Himanen, D. Kunz, M. J. Barbanjo, J. Roschke, A. Varri, and G. Dorffner, *IEEE Eng. Med. Biol. Mag.* **20**, 51 (2001); H. Danker-Hopfe *et al.*, *J. Sleep Res.* **13**, 63 (2004).
- ²⁶J. M. Ernst, D. A. Litvack, D. L. Lozano, J. T. Cacioppo, and G. G. Berntson, *Psychophysiology* **36**, 333 (1999); J. H. Houtveen, P. F. C. Groot, and E. J. C. de Geus, *Int. J. Psychophysiol.* **59**, 97 (2006).
- ²⁷Polysomnography: specific physiologic variables are continuously recorded during sleep. Commonly, polysomnographic recordings include heart beat data (electrocardiogram=EKG), respiration (tidal volume, timing of breathing), brain wave recordings (multiple lead electroencephalogram=EEG), eye movements (electrooculogram=EOG), muscle tone (electromyogram=EMG), and leg movements.
- ²⁸J. A. Hirsch and B. Bishop, *Am. J. Physiol.* **241**, H620 (1981); T. E. Brown, L. A. Beightol, J. Koh, and D. L. Eckberg, *J. Appl. Physiol.* **75**, 2310 (1993); J. Penttilä, A. Helminen, T. Jartti, T. Kuusela, H. V. Huikuri, M. P. Tulppo, R. Coffeng, and H. Scheinin, *Clin. Physiol.* **21**, 365 (2001).
- ²⁹American Academy of Sleep Medicine Task Force, *Sleep* **22**, 667 (1999).
- ³⁰Available on the internet at www.librasch.org.
- ³¹B. U. Köhler, C. Hennig, and R. Orglmeister, *IEEE Eng. Med. Biol. Mag.* **21**, 42 (2002).
- ³²D. Gabor, *J. Inst. Electr. Eng.* **93**, 429 (1946).
- ³³B. Boashash, *Proc. IEEE* **80**, 520 (1992); **80**, 540 (1992).
- ³⁴D. Hoyer, U. Leder, H. Hoyer, B. Pompe, M. Sommer, and U. Zwiener, *Med. Eng. Phys.* **24**, 33 (2002).